ARTICLES

Locally dynamic synaptic learning rules in pyramidal neuron dendrites

Christopher D. Harvey[1,2] & Karel Svoboda[1,2]

Long-term potentiation (LTP) of synaptic transmission underlies aspects of learning and memory. LTP is input-specific at the level of individual synapses, but neural network models predict interactions between plasticity at nearby synapses. Here we show in mouse hippocampal pyramidal cells that LTP at individual synapses reduces the threshold for potentiation at neighbouring synapses. After input-specific LTP induction by two-photon glutamate uncaging or by synaptic stimulation, subthreshold stimuli, which by themselves were too weak to trigger LTP, caused robust LTP and spine enlargement at neighbouring spines. Furthermore, LTP induction broadened the presynaptic–postsynaptic spike interval for spike-timing-dependent LTP within a dendritic neighbourhood. The reduction in the threshold for LTP induction lasted ~10 min and spread over ~10 μm of dendrite. These local interactions between neighbouring synapses support clustered plasticity models of memory storage and could allow for the binding of behaviourally linked information on the same dendritic branch.

Long-lasting modifications of synaptic strength (LTP) are critical for learning and memory in many parts of the brain, including the hippocampus[1]. The extent to which LTP is synapse-specific influences the information processing and storage of a neuron. LTP can be input-specific[2], even at the level of individual synapses[3], indicating that synapses may function as independent units of plasticity[4]. However, neighbouring synapses might be co-regulated due to the heterosynaptic spread of LTP over short stretches of dendrite[5].

Neural network models predict interactions between plasticity at nearby synapses. Heterosynaptic metaplasticity suggests that LTP at one set of synapses may subsequently increase the threshold for potentiation at other synapses[6,7]. In contrast, clustered plasticity models[8–10] predict a decrease in the threshold for LTP in the neighbourhood of recently potentiated synapses, for example, owing to local synaptic tagging[10–12]. To distinguish between these possibilities, we probed the coupling between plasticity at nearby synapses using two-photon glutamate uncaging[3,13–16] combined with two-photon laser scanning microscopy[17,18] and perforated patch whole-cell recordings of synaptic currents.

Crosstalk between plasticity at nearby synapses

Does LTP at one synapse influence the threshold for plasticity at neighbouring synapses? We looked for such 'crosstalk' in acute hippocampal slices from green fluorescent protein (GFP)-expressing transgenic mice[19]. Dendritic spines were imaged on proximal (distance to the soma, <100 μm) secondary and tertiary apical dendrites of CA1 pyramidal neurons (Fig. 1a, c, e). Glutamate receptors on individual spines were stimulated with two-photon glutamate uncaging, and the resulting uncaging-evoked excitatory postsynaptic currents (uEPSCs) were measured at the soma using perforated patch-clamp recordings.

To induce LTP at individual spines, we paired a train of 30 stimuli (0.5 Hz) with postsynaptic depolarization to ~0 mV (ref. 3). In this 'LTP protocol', each uncaging stimulus (4 ms duration) triggered NMDA-R (*N*-methyl-D-aspartate receptor)-mediated spine $[Ca^{2+}]$ accumulations that were similar to $[Ca^{2+}]$ transients evoked by low-frequency synaptic stimulation at 0 mV (ref. 20) or by tetanic stimulation[21] (Supplementary Fig. 1b, c; see Supplementary Information). $[Ca^{2+}]$ accumulations were restricted to the stimulated spine (Supplementary Fig. 1a–c), indicating that glutamate did not spread to activate neighbouring spines. As a readout of plasticity, we monitored spine volumes and uEPSCs in response to test stimuli at the spine receiving the LTP protocol (LTP spine) and at neighbouring spines less than 4 μm from the LTP spine on the same branch. The LTP protocol resulted in a long-lasting (>40 min) increase in uEPSC amplitude and spine volume (Vol) at the LTP spine, but not at nearby spines ($\Delta uEPSC_{LTP\ spine} = 99 \pm 17\%$ (mean ± s.e.m.), $P < 0.01$; $\Delta uEPSC_{nearby\ spine} = -1 \pm 9\%$, $P > 0.9$; $\Delta Vol_{LTP\ spine} = 78 \pm 10\%$, $P < 0.01$; $\Delta Vol_{nearby\ spines} = 0 \pm 4\%$, $P > 0.9$; Fig. 1a, b). A similar protocol, but in which the amplitudes of NMDA-R-mediated spine $[Ca^{2+}]$ transients were reduced by a factor of four (subthreshold protocol, 1-ms pulse duration; Supplementary Fig. 1b, c), did not change uEPSC amplitude or spine volume at the spine receiving the uncaging stimuli (sub spine) or at nearby spines ($\Delta uEPSC_{sub\ spine} = -1 \pm 2\%$, $P > 0.4$; $\Delta uEPSC_{nearby\ spine} = 2 \pm 2\%$, $P > 0.6$; $\Delta Vol_{sub\ spine} = 1 \pm 1\%$, $P > 0.6$; $\Delta Vol_{nearby\ spines} = 1 \pm 4\%$, $P > 0.8$; Fig. 1c, d).

To test for crosstalk, we induced LTP at one spine (LTP spine) and, 90 s later, provided the subthreshold protocol at a neighbouring spine (sub spine). The subthreshold protocol now triggered LTP and a long-lasting spine enlargement ($\Delta uEPSC_{LTP\ spine} = 95 \pm 11\%$, $P < 0.01$; $\Delta uEPSC_{sub\ spine} = 97 \pm 10\%$, $P < 0.01$; $\Delta Vol_{LTP\ spine} = 76 \pm 16\%$, $P < 0.02$; $\Delta Vol_{sub\ spine} = 81 \pm 10\%$, $P < 0.01$; Fig. 1e, f). The levels of functional and structural plasticity were similar in spines receiving the LTP and subthreshold protocols (uEPSC, $P > 0.5$; Vol, $P > 0.5$; Fig. 1g). Other nearby spines that received neither stimulus did not change ($\Delta Vol = 1 \pm 1\%$, $P > 0.7$). Crosstalk did not occur after application of the LTP protocol at a postsynaptic potential of approximately −70 mV, which did not induce LTP, arguing that crosstalk is triggered by LTP induction and not by the uncaging process itself (see Supplementary Information). LTP induction at one spine therefore lowered the threshold for potentiation at nearby spines while maintaining input specificity.

[1]Janelia Farm Research Campus, HHMI, Ashburn, Virginia 20147, USA. [2]Watson School of Biological Sciences, Cold Spring Harbor Laboratory, Cold Spring Harbor, New York 11724, USA.

The changes in uEPSC amplitude and spine volume were highly correlated[3,22] ($r = 0.86$, $P < 0.0001$; Fig. 1h), consistent with documented relationships between spine volume, postsynaptic density area and the number of AMPA (α-amino-3-hydroxy-5-methyl-4-isoxazole propionic acid) receptors in the postsynaptic density[14,23,24]. These observations confirm that spine enlargement is a structural correlate of LTP[3,22].

Crosstalk in unperturbed neurons

The pairing LTP protocol (Fig. 1) has non-physiological features. For example, depolarization of the postsynaptic neuron during pairing causes global Ca^{2+} influx through voltage-gated calcium channels, which could contribute to the crosstalk between synapses. To test if crosstalk occurs without sustained postsynaptic depolarization, we stimulated NMDA-Rs on individual spines from unperturbed neurons (in nominally 0 mM Mg^{2+}). Uncaging stimuli triggered $[Ca^{2+}]$ transients that were restricted to the activated spine (Supplementary Fig. 1a–c). Each uncaging pulse during the LTP protocol produced NMDA-R currents (7.9 ± 1.1 pA; Supplementary Fig. 1a, d) that corresponded to the opening of ~5 NMDA-Rs, comparable to the number of receptors opened by low-frequency synaptic stimulation[25]. The LTP protocol triggered a large transient increase in spine volume in the LTP spine that decayed to a persistent spine enlargement after 10 min; spines neighbouring the stimulated spine did not change ($\Delta Vol_{LTP\ spine} = 76 \pm 18\%$, $P < 0.01$; $\Delta Vol_{nearby\ spines} = -1 \pm 4\%$, $P > 0.7$; Fig. 2b, e, f). The subthreshold protocol, which produced approximately fourfold lower NMDA-R currents and $[Ca^{2+}]$ accumulations (Supplementary Fig. 1a–d), triggered only transient changes in spine volume that decayed within 10 min ($\Delta Vol_{sub\ spine} = 5 \pm 6\%$, $P > 0.3$; Fig. 2c, e, f). We next provided the LTP protocol at one spine and, 90 s later, tested for crosstalk by applying the subthreshold protocol at a neighbouring spine. The subthreshold protocol now induced sustained spine enlargement of the same size as that induced by the LTP protocol ($\Delta Vol_{LTP\ spine} = 66 \pm 8$ %, $P < 0.0001$; $\Delta Vol_{sub\ spine} = 67 \pm 10\%$, $P < 0.0001$; LTP spine versus sub spine, $P > 0.95$; Fig. 2d–f). Other spines that received neither stimulus did not change ($\Delta Vol = 0 \pm 1\%$, $P > 0.95$). Similar results were obtained in cultured rat hippocampal slices (Supplementary Fig. 2a–d). Persistent postsynaptic depolarization therefore was not required to observe the crosstalk in plasticity between synapses.

Crosstalk with synaptically induced plasticity

Glutamate released by uncaging may activate a distinct set of receptors compared to synaptically released glutamate. We therefore tested if crosstalk occurs after synaptically induced plasticity. Schaffer collateral axons were stimulated (120 pulses, 2 Hz) in low extracellular Mg^{2+} (refs 3 and 26). This 'synaptic LTP protocol' induced long-lasting spine enlargement in a sparse subset of spines (see Methods). The magnitude of the spine volume change ($\Delta Vol_{synaptic\ LTP\ spine} =$

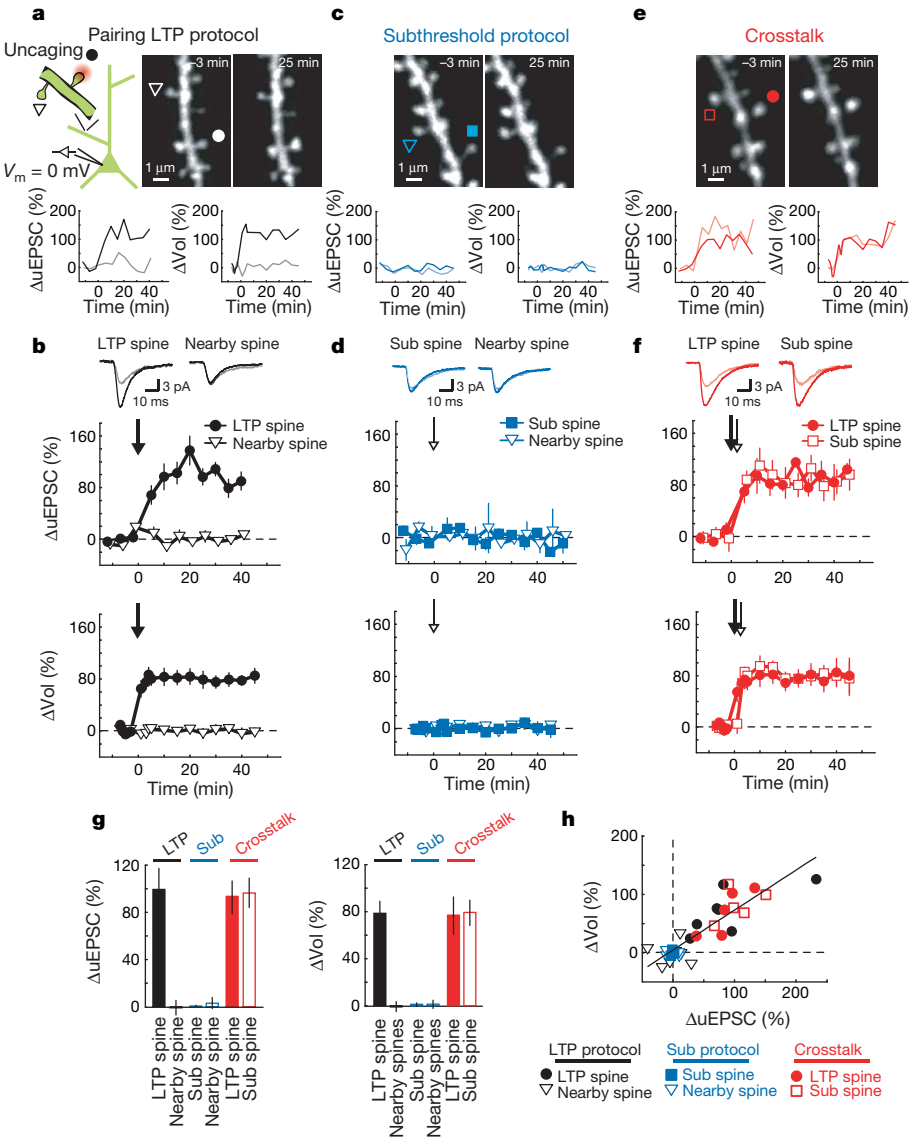

Figure 1 | Crosstalk with pairing-induced LTP. **a**, Top left, schematic of the experiment. V_m, membrane potential. Right, images before (−3 min) and after (25 min) LTP induction. At time = 0 the LTP protocol (30 uncaging pulses at 0.5 Hz, 4-ms pulse duration, postsynaptic potential 0 mV) was applied to the spine marked by a circle (LTP spine). A triangle marks a tested nearby spine. Lower panels show changes in uEPSC amplitude and spine volume at the LTP (black) and nearby (grey) spines. **b**, Upper panels, uEPSCs, averaged across all cells, in response to test stimuli before (−3 min; grey) and after (40 min; black) the LTP protocol. Lower panels, time course of the changes in uEPSC amplitude and spine volume at the LTP spine (filled circles; $n = 7$) and at nearby spines (open triangles; uEPSC, $n = 7$; Vol, $n = 31$). The arrow marks the LTP protocol. **c**, **d**, Same as for **a** and **b** except with the subthreshold protocol. At time = 0 the subthreshold protocol (30 uncaging pulses at 0.5 Hz, 1-ms pulse duration, postsynaptic potential 0 mV) was applied to the spine marked by a filled square (sub spine; $n = 5$). Open triangles indicate nearby spines (uEPSC, $n = 5$; Vol, $n = 26$). **e**, **f**, Same as for **a** and **b**, except for the crosstalk case. At time = 0 the LTP protocol was applied to the spine marked by a filled circle (LTP spine) and, 90 s later, the subthreshold protocol was given at the spine marked by an open square (sub spine). $n = 5$, mean ± s.e.m. **g**, Changes in uEPSC amplitude and spine volume. Error bars indicate mean ± s.e.m. **h**, Correlation between changes in uEPSC amplitude and spine volume. $r = 0.86$, $P < 0.0001$.

70 ± 14%, $P < 0.001$) was similar to that triggered by the uncaging LTP protocol[3] ($P > 0.8$; compare Fig. 3e and Fig. 2b). Spine enlargement was thus used to identify synapses potentiated by synaptic stimulation (see Methods). To test for crosstalk, we provided the subthreshold protocol at a nearby spine (sub spine) two minutes after the synaptic LTP protocol. The subthreshold protocol, which by itself did not trigger structural plasticity (Fig. 2c, e, f), now induced a persistent spine enlargement ($\Delta Vol_{sub\ spine} = 62 \pm 9\%$, $P < 0.001$) of similar magnitude to the synaptically induced volume change ($P > 0.6$; Fig. 3b–e). Other nearby spines did not change ($\Delta Vol_{nearby\ spines} = -3 \pm 5\%$, $P > 0.4$; Fig. 3b–e). Synaptically induced plasticity therefore reduced the threshold for potentiation at neighbouring synapses.

Modulation of the window for STDP

Excitatory postsynaptic potentials (EPSPs) followed by action potentials within a short time window (tens of milliseconds) can trigger LTP[27]. The magnitude of this spike-timing-dependent potentiation (STDP) decreases monotonically with the time between the EPSP and the action potential[28,29]. Because crosstalk reduces the threshold for potentiation in the neighbourhood of the LTP spine, crosstalk could broaden the spike time window (Δt) for STDP at neighbouring spines. We induced STDP with uncaging pulses (60 pulses, 2 Hz) followed ($\Delta t = 5$ ms) by three action potentials at 50 Hz. The amplitudes of uEPSPs (0.41 ± 0.19 mV, mean ± s.d.) were similar to those of miniature EPSPs[30]. This induction protocol induced long-lasting increases in the uEPSC amplitude and spine volume at the stimulated spine, but not at nearby spines within 4 µm on the same dendritic branch ($\Delta uEPSC_{\Delta t = 5\ ms} = 62 \pm 17\%$, $P < 0.02$; $\Delta uEPSC_{nearby\ spine} = 5 \pm 8\%$, $P > 0.5$; $\Delta Vol_{\Delta t = 5\ ms} = 57 \pm 13\%$, $P < 0.01$; $\Delta Vol_{nearby\ spines} = 0 \pm 3\%$, $P > 0.8$; Fig. 4b, d). The magnitudes of functional and structural plasticity decreased as the time between the uEPSP and the action potentials increased ($\tau_{\Delta uEPSC} = 17.6$ ms; $\tau_{\Delta Vol} = 16.6$ ms; Fig. 4c). Pairing at longer intervals ($\Delta t = 35$ ms) did not trigger LTP or spine enlargement ($\Delta uEPSC_{\Delta t = 35\ ms} = -3 \pm 10\%$, $P > 0.8$; $\Delta Vol_{\Delta t = 35\ ms} = 4 \pm 3\%$, $P > 0.2$; Fig. 4e), indicating that uEPSPs or action potentials alone were not sufficient to trigger LTP. STDP therefore was induced at single spines in an input-specific manner.

We next induced STDP at one spine with an uEPSP-to-action-potential time window of 5 ms, and, 90 s later, stimulated a

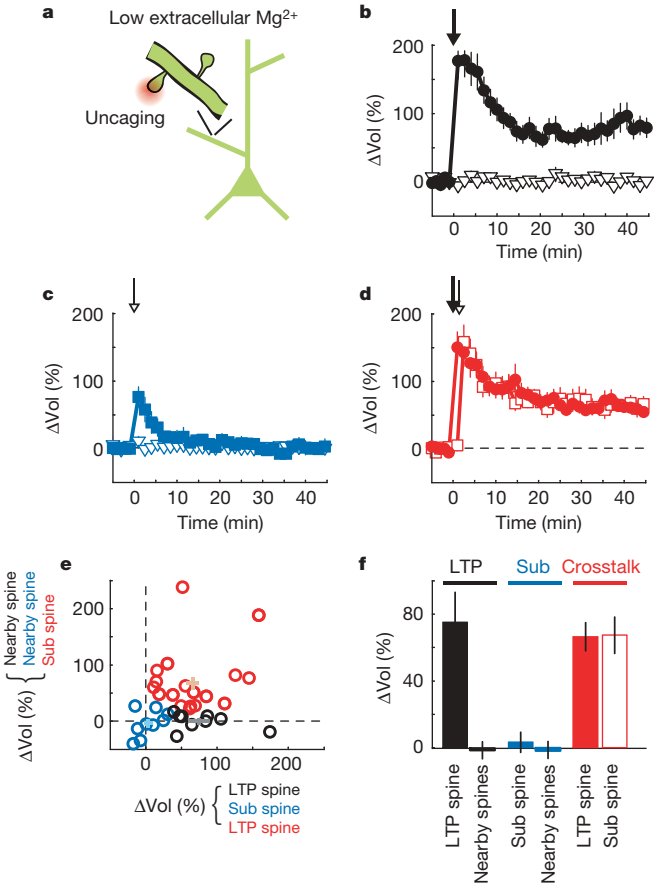

Figure 2 | Crosstalk in unperturbed neurons. **a**, Schematic of the experiment. **b**, Time course of the spine-volume changes induced by the LTP protocol (applied at time = 0, 30 uncaging pulses at 0.5 Hz, 4-ms pulse duration, in low extracellular Mg^{2+}) for the stimulated spine (LTP spine, closed circles; $n = 9$) and nearby spines (open triangle; $n = 29$). **c**, Time course of the spine-volume changes induced by the subthreshold protocol (applied at time = 0, 30 uncaging pulses at 0.5 Hz, 1-ms pulse duration, in low extracellular Mg^{2+}) for the stimulated spine (sub spine, filled squares; $n = 8$) and nearby spines (open triangles; $n = 38$). **d**, Time course of the spine-volume changes for the crosstalk case. At time = 0 the LTP protocol was applied to the LTP spine (filled circles) and, 90 s later, the subthreshold protocol was given at a neighbouring spine (sub spine, open squares). $n = 18$, mean ± s.e.m. **e**, Spine volume changes from individual experiments. Black, LTP protocol; blue, sub protocol; red, crosstalk. Crosses indicate mean ± s.e.m. **f**, Changes in spine volume. Error bars indicate mean ± s.e.m.

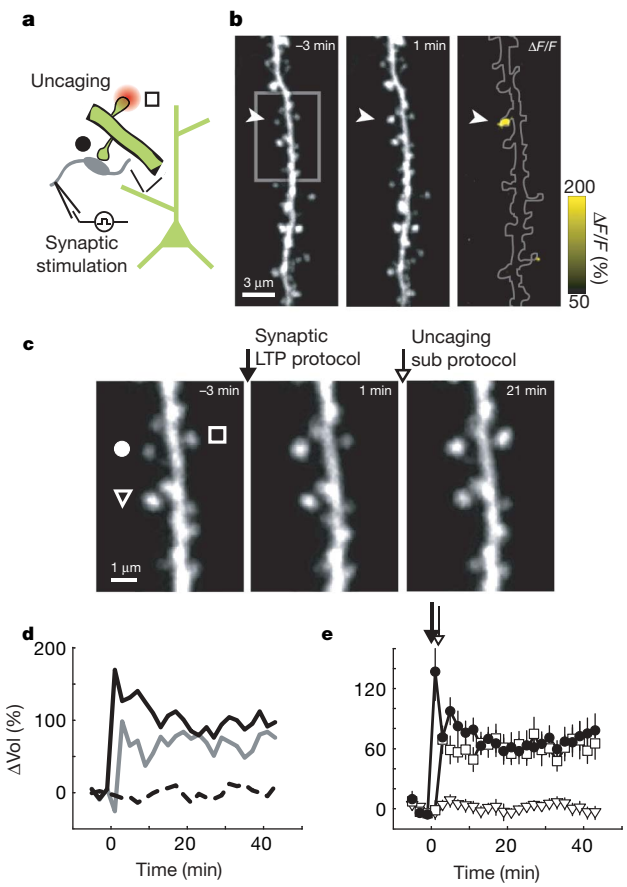

Figure 3 | Crosstalk with synaptically induced plasticity. **a**, Schematic of the experiment. **b**, Images before (−3 min) and after (1 min) the synaptic LTP protocol (applied at time = 0; 120 stimuli, 2 Hz in low extracellular Mg^{2+}). The arrowheads mark an enlarged spine (synaptic LTP spine). A ratio image ($\Delta F/F$) comparing fluorescence intensity before (−3 min) and after (1 min) the synaptic LTP protocol is shown. **c**, High magnification images before stimulation (−3 min), after the synaptic LTP protocol (1 min; applied at time = 0), and after the subthreshold protocol (21 min; applied at time = 2 min). The circle, square and triangle mark the synaptic LTP spine, the sub spine and a nearby spine, respectively. **d**, Changes in spine volume for the example shown in **b** and **c**. Black solid line, synaptic LTP spine; grey solid line, sub spine; black dashed line, nearby spine. **e**, Time course of the change in spine volume for synaptic LTP spines (filled circle; $n = 11$), sub spines (open square; $n = 11$) and nearby spines (open triangle; $n = 34$), mean ± s.e.m.

neighbouring spine with an uEPSP–action potential interval of 35 ms. Under these conditions, the uEPSP–action potential pairing at the 35-ms time window now induced LTP and a long-lasting spine enlargement ($\Delta uEPSC_{\Delta t=5\,ms} = 67 \pm 10\%$, $P < 0.01$; $\Delta uEPSC_{\Delta t=35\,ms} = 69 \pm 8\%$, $P < 0.01$; $\Delta Vol_{\Delta t=5\,ms} = 68 \pm 9\%$, $P < 0.01$; $\Delta Vol_{\Delta t=35\,ms} = 74 \pm 15\%$, $P < 0.02$; Fig. 4f). The levels of functional and structural plasticity were similar in spines receiving the pairing at short and long intervals (uEPSC, $P > 0.4$; Vol, $P > 0.4$; Fig. 4g), and the changes in uEPSC amplitude and spine volume were highly correlated ($r = 0.81$, $P < 0.0001$; Fig. 4h). Other nearby spines that received neither stimulus did not change ($\Delta Vol = -1 \pm 1\%$, $P > 0.7$). LTP induction at one spine therefore broadened the uEPSP–action potential time window for STDP at neighbouring spines.

Characterization of crosstalk

We next measured the timescale of the crosstalk in plasticity between synapses. We varied the time between the LTP and subthreshold protocols given in low extracellular Mg^{2+} while maintaining the distance between the stimulated spines at ~3 μm. The crosstalk was measured as the volume change triggered by the subthreshold protocol at the sub spine after LTP induction at the LTP spine. Crosstalk decreased gradually with time and lasted for up to 10 min ($t_{1/2} = 5.3$ min; Fig. 5a).

To determine the length scale of the crosstalk, we varied the distance between the spines receiving the LTP and subthreshold protocols while keeping the time between stimuli at 90 s. Crosstalk decreased gradually with distance for up to ~8 μm in both directions along the parent dendrite (full-width at half-maximum = 11.1 μm; Fig. 5b). The magnitude of crosstalk was similar for spines farther or closer to the apical trunk with respect to the spine receiving the LTP protocol (data not shown). The length scale of the crosstalk was similar in cultured rat hippocampal slices (full-width at half-maximum = 10.2 μm; Supplementary Fig. 2e). Consistently, when spines separated by ~10 μm were stimulated by the LTP and subthreshold protocols paired with depolarization to ~0 mV, the subthreshold protocol did not induce functional or structural plasticity ($\Delta uEPSC_{sub\ spine} = -7 \pm 5\%$, $P > 0.15$; $\Delta Vol_{sub\ spine} = -8 \pm 8\%$, $P > 0.4$; Fig. 5c). Furthermore, after synaptically induced spine enlargement, the subthreshold protocol did not trigger structural plasticity at spines located ~10 μm from the enlarged spine ($\Delta Vol_{sub\ spine} = -3 \pm 8\%$, $P > 0.9$; Fig. 5d).

Our experiments indicate that LTP induction activates a factor at the LTP spine that spreads to reduce the threshold for potentiation at neighbouring synapses. Extracellular diffusible factors have been implicated in the heterosynaptic spread of LTP[31,32]. Similarly, intracellular factors can spread over the relevant time and length scales[33,34] (C.D.H., Ryohei Yasuda and K.S., unpublished). To distinguish between extracellular and intracellular factors, we examined whether crosstalk can occur between spines that are close within the neuropil (<4 μm) but are located on different dendritic branches and therefore are far apart in terms of cytoplasmic distance (>50 μm). We induced LTP at one spine and, 90 s later, provided the subthreshold protocol at the sub spine less than 4 μm away on a nearby dendritic branch from the same cell. Under these conditions, the subthreshold

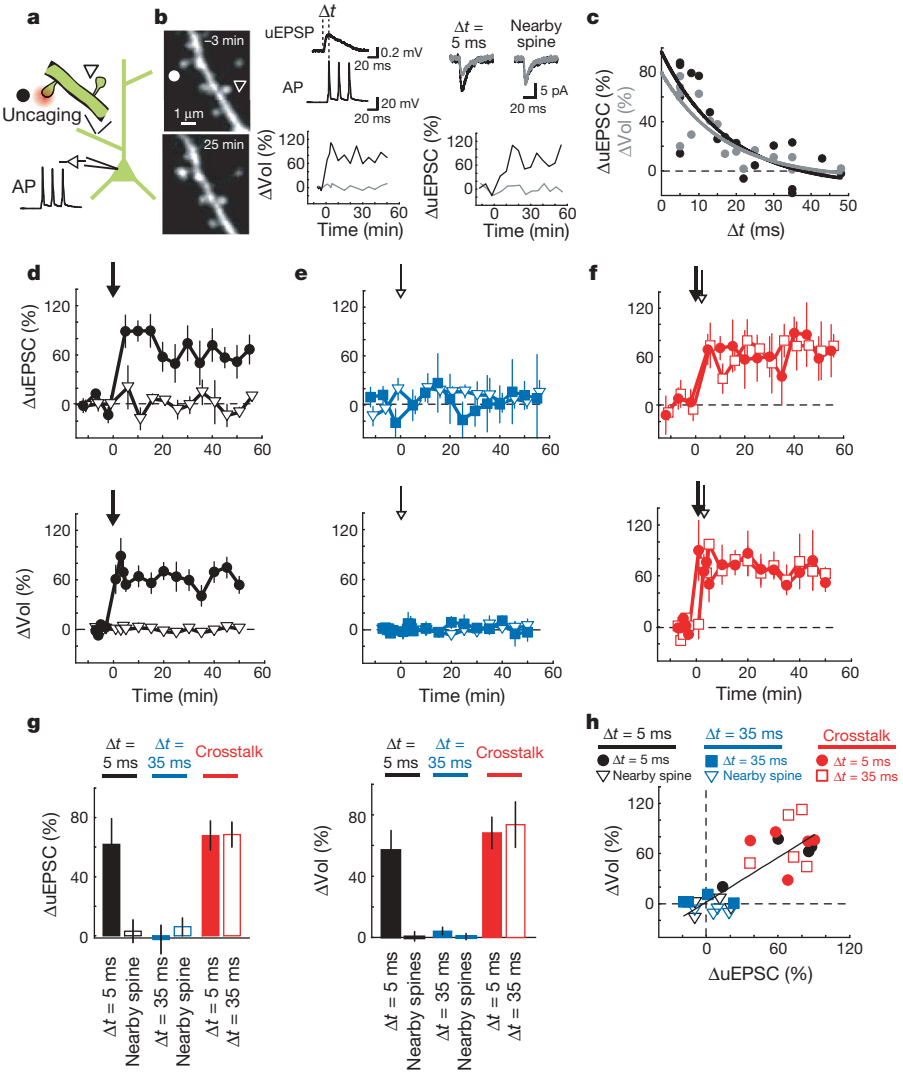

Figure 4 | Crosstalk with spike-timing-dependent LTP. **a**, Schematic of the experiment. **b**, Left, images before (−3 min) and after (25 min) spike-timing-dependent LTP induction. At time = 0, uncaging pulses (60 pulses at 2 Hz) followed by three action potentials at 50 Hz ($\Delta t = 5$ ms) were applied to the spine marked by the circle. The triangle marks a tested nearby spine. Top middle, example uEPSPs and action potentials (APs) from unpaired stimuli. Top right, uEPSCs averaged over 5 trials before (−6 min, grey line) and after (25 min, black line) uEPSP–action potential pairing. Bottom middle and bottom right, changes in uEPSC amplitude and spine volume at the stimulated (black) and nearby (grey) spines. **c**, Changes in uEPSC amplitude (black) and spine volume (grey) at different uEPSP–action potential time windows (Δt). Changes were measured from 20–30 min post stimulus. Exponential fits are shown. **d**, Time course of the changes in uEPSC amplitude and spine volume for uEPSP–action potential pairing at $\Delta t = 5$ ms (filled circle; $n = 4$) and at nearby spines (open triangle; uEPSC, $n = 4$; Vol, $n = 20$). The arrow marks the time of uEPSP–action potential pairing. **e**, Time course of the changes in uEPSC amplitude and spine volume for uEPSP–action potential pairing at $\Delta t = 35$ ms (filled square; $n = 4$) and at nearby spines (open triangle; uEPSC, $n = 4$; Vol, $n = 21$). **f**, Time course of the changes in uEPSC amplitude and spine volume for the crosstalk case. At time = 0, one spine was stimulated with uEPSP–action potential pairing at $\Delta t = 5$ ms (filled circle) and, 90 s later, a neighbouring spine was stimulated with uEPSP–action potential pairing at $\Delta t = 35$ ms (open square). $n = 5$, mean ± s.e.m. **g**, Changes in uEPSC amplitude and spine volume. Error bars indicate mean ± s.e.m. **h**, Correlation between changes in uEPSC amplitude and spine volume. $r = 0.81$, $P < 0.0001$.

protocol failed to induce structural plasticity ($\Delta Vol_{sub\ spine} = 1 \pm 9\%$, $P > 0.6$; Fig. 6a), indicating that intracellular factors, rather than extracellular factors, were necessary for the crosstalk between synapses.

Ca^{2+} release from intracellular stores has been implicated in the heterosynaptic spread of some forms of synaptic plasticity[35,36]. However, eliminating Ca^{2+} release from intracellular stores using thapsigargin (1 μM) and ryanodine (20 μM) (Supplementary Fig. 3) did not affect the crosstalk between synapses ($\Delta Vol_{sub\ spine} = 67 \pm 19\%$, $P > 0.95$) (Fig. 6b).

The crosstalk in plasticity between neighbouring synapses described here shares characteristics with synaptic tagging, in which early LTP at one set of synapses can be converted into late LTP by the strong stimulation of a second group of synapses[11]. Synaptic-tagging-based plasticity occurs both when the 'weak' stimulus precedes and when it follows the 'strong' stimulus[37,38]. We therefore tested if the crosstalk in plasticity depends on the order of stimuli. When the subthreshold protocol preceded the LTP protocol by 90 s, the subthreshold protocol did not induce spine enlargement ($\Delta Vol_{sub\ spine} = 2 \pm 14\%$, $P > 0.8$; Fig. 5a). Because synaptic-tagging-based crosstalk requires the capture of newly synthesized proteins[11,39], we also tested the role of protein synthesis in the crosstalk between neighbouring synapses. Application of the protein synthesis inhibitor anisomycin (25 μM) had no effect on the spine enlargement induced by the LTP and subthreshold protocols ($\Delta Vol_{LTP\ spine} = 63 \pm 11\%$, $P > 0.7$; $\Delta Vol_{sub\ spine} = 79 \pm 17\%$, $P > 0.3$; Fig. 6b). Similar results were obtained with other protein synthesis inhibitors (60 μM cycloheximide, $\Delta Vol_{sub\ spine} = 64 \pm 16\%$, $P > 0.9$; 50 μM emetine, $\Delta Vol_{sub\ spine} = 78 \pm 8\%$, $P > 0.6$). As a positive control for inhibitor function, anisomycin, cycloheximide and emetine caused a rapid decrease in destabilized EGFP fluorescence[40] (Supplementary Fig. 4). The crosstalk in plasticity between neighbouring spines is therefore distinct from synaptic tagging.

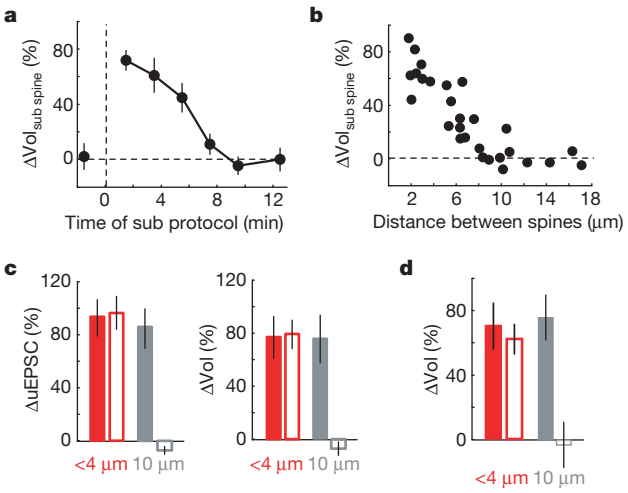

Figure 5 | Spatial and temporal scales of crosstalk. **a**, Timescale of crosstalk. At time = 0, the LTP protocol was applied to a single spine (in low extracellular Mg^{2+}, see Fig. 2). The subthreshold protocol was applied to a neighbouring spine (sub spine) ~3 μm away. $n \geq 4$ for all time points, mean ± s.e.m. **b**, Length scale of crosstalk. The LTP protocol was applied to a single spine and, 90 s later, a nearby spine (sub spine) was stimulated with the subthreshold protocol (in low extracellular Mg^{2+}, see Fig. 2). **c**, Distance-dependence of crosstalk with pairing-induced plasticity. The LTP protocol (at postsynaptic potential 0 mV) was applied to the LTP spine and, 90 s later, the subthreshold protocol (at postsynaptic potential 0 mV) was applied to a spine (sub spine) either less than 4 μm or ~10 μm away (see Fig. 1). The data for spines separated by less than 4 μm are from Fig. 1. $n = 4$ at 10 μm, mean ± s.e.m. Filled bars, LTP spine; open bars, sub spine. **d**, Distance-dependence of crosstalk with synaptically induced plasticity. The synaptic LTP protocol was applied in low extracellular Mg^{2+} to induce plasticity in the synaptic LTP spine. Two minutes later, the subthreshold protocol was applied to a spine (sub spine) either less than 4 μm or ~10 μm away (see Fig. 3). The data for spines separated by less than 4 μm are from Fig. 3. $n = 5$ at 10 μm, mean ± s.e.m. Filled bars, synaptic LTP spine; open bars, sub spine.

Discussion

We have shown that the induction of plasticity at individual synapses can be influenced by events at neighbouring synapses. LTP induction at one synapse decreased the threshold for potentiation at nearby synapses within ~10 μm for ~10 min. Crosstalk did not perturb input-specificity *per se*, and therefore differed from the heterosynaptic spread of plasticity[5,31,32,35]. However, the reduction in LTP induction threshold in the vicinity of a potentiated synapse may help explain discrepancies between data showing the heterosynaptic spread of LTP[5] and synapse-specific LTP at single spines[3]. Previous studies have suggested that synaptic plasticity can be influenced by prior neural activity[6,7,11,12,41–43]. However, the time courses of these interactions were much longer than the timescale of crosstalk reported here. Furthermore, these studies did not establish a length scale for crosstalk.

What cellular mechanisms could underlie the crosstalk in plasticity between neighbouring synapses? Our results indicate that the intersynaptic spread of intracellular signalling factors probably has a key role. The timescale and spatial scale of crosstalk are consistent with a diffusing cytoplasmic factor[33,34]. This factor could modify synaptic properties at nearby spines to decrease the threshold for LTP or may provide enzymatic activity that is necessary for LTP induction but is not produced by subthreshold stimuli.

Although synaptic modifications can occur in an input-specific manner[3] (Figs 1a, b, 2b and 4d), the coordinated regulation of groups of 10–20 synapses within a dendritic neighbourhood indicates that individual synapses do not necessarily function as independent units of plasticity. Models of clustered plasticity[8–10] propose that individual engrams could be stored in synapses sharing the same dendritic branch, which would increase the information storage capacity of the neuron through the nonlinear summation of synaptic inputs[8,9,30,44]. Clustered plasticity implies the binding of inputs that are active during the same behavioural epochs on the same dendritic branch. It will be of interest to map the distribution of the information carried by synapses within the dendritic trees of individual neurons.

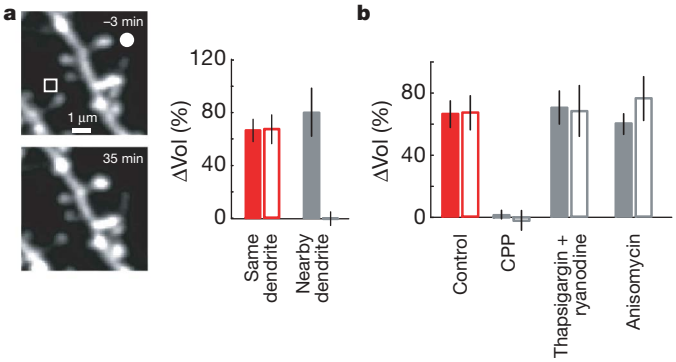

Figure 6 | Signalling underlying crosstalk. **a**, Crosstalk examined at nearby dendritic branches. The LTP protocol was applied to the spine marked by a circle (LTP spine) and, 90 s later, the subthreshold protocol was given at a spine on a nearby dendritic branch from the same cell (sub spine, square; in low extracellular Mg^{2+}, see Fig. 2). Example images are shown. The 'same dendrite' data are from Fig. 2. $n = 5$ for nearby dendrites, mean ± s.e.m. Filled bars, LTP spine; open bars, sub spine. **b**, Pharmacological analysis of crosstalk. In the presence of the specified drugs, the LTP protocol was applied to the LTP spine and, 90 s later, a neighbouring spine (sub spine) was stimulated with the subthreshold protocol (in low extracellular Mg^{2+}, see Fig. 2). Control data are from Fig. 2. $n = 4$ each for CPP (3-(*R*-2-carboxypiperazin-4-yl)-propyl-1-phosphonic acid; 10 μM), thapsigargin (1 μM) + ryanodine (20 μM), and anisomycin (25 μM), mean ± s.e.m. Filled bars, LTP spine; open bars, sub spine.

METHODS SUMMARY

Acute hippocampal brain slices were prepared from Thy1 GFP mice[19] (line M; postnatal day 14–18). Two-photon laser-scanning microscopy and two-photon glutamate uncaging were performed using a custom-built microscope with two Ti:sapphire lasers. For glutamate uncaging, brief (1 or 4 ms) laser exposures were delivered ~0.5 μm from the tip of the spine head in the presence of 2.5 mM methoxy-nitroindoline(MNI)-caged-L-glutamate. Uncaging-evoked EPSCs (uEPSCs) were measured using amphotericin-mediated perforated patch-clamp recordings. For synaptic stimulation (Fig. 3), short current pulses (0.1 ms, 30 μA) were delivered with a glass pipette positioned close (10 to 20 μm) to a GFP-labelled dendrite of interest. Plasticity was induced using four protocols: depolarization to ~0 mV paired with 30 uncaging pulses at 0.5 Hz (Fig. 1); 30 uncaging pulses at 0.5 Hz in low extracellular Mg^{2+} (Fig. 2); 120 synaptic stimuli at 2 Hz in low extracellular Mg^{2+} (Fig. 3); and an uncaging pulse followed by three action potentials at 50 Hz, repeated 60 times at 2 Hz (Fig. 4). Spine volumes were measured as the integrated green fluorescence after background subtraction, which is proportional to spine volume[45], normalized to the fluorescence intensity of the thick apical dendrite[25].

Full Methods and any associated references are available in the online version of the paper at www.nature.com/nature.

Received 12 August; accepted 29 October 2007.

1. Malenka, R. C. & Bear, M. F. LTP and LTD: an embarrassment of riches. *Neuron* **44,** 5–21 (2004).
2. Andersen, P., Sundberg, S. H., Sveen, O. & Wigstrom, H. Specific long-lasting potentiation of synaptic transmission in hippocampal slices. *Nature* **266,** 736–737 (1977).
3. Matsuzaki, M., Honkura, N., Ellis-Davies, G. C. & Kasai, H. Structural basis of long-term potentiation in single dendritic spines. *Nature* **429,** 761–766 (2004).
4. Yuste, R. & Denk, W. Dendritic spines as basic functional units of neuronal integration. *Nature* **375,** 682–684 (1995).
5. Engert, F. & Bonhoeffer, T. Synapse specificity of long-term potentiation breaks down at short distances. *Nature* **388,** 279–284 (1997).
6. Abraham, W. C., Mason-Parker, S. E., Bear, M. F., Webb, S. & Tate, W. P. Heterosynaptic metaplasticity in the hippocampus *in vivo*: a BCM-like modifiable threshold for LTP. *Proc. Natl Acad. Sci. USA* **98,** 10924–10929 (2001).
7. Wang, H. & Wagner, J. J. Priming-induced shift in synaptic plasticity in the rat hippocampus. *J. Neurophysiol.* **82,** 2024–2028 (1999).
8. Poirazi, P. & Mel, B. W. Impact of active dendrites and structural plasticity on the memory capacity of neural tissue. *Neuron* **29,** 779–796 (2001).
9. Mehta, M. R. Cooperative LTP can map memory sequences on dendritic branches. *Trends Neurosci.* **27,** 69–72 (2004).
10. Govindarajan, A., Kelleher, R. J. & Tonegawa, S. A clustered plasticity model of long-term memory engrams. *Nature Rev. Neurosci.* **7,** 575–583 (2006).
11. Frey, U. & Morris, R. G. Synaptic tagging and long-term potentiation. *Nature* **385,** 533–536 (1997).
12. Martin, K. C. *et al.* Synapse-specific, long-term facilitation of aplysia sensory to motor synapses: a function for local protein synthesis in memory storage. *Cell* **91,** 927–938 (1997).
13. Furuta, T. *et al.* Brominated 7-hydroxycoumarin-4-ylmethyls: photolabile protecting groups with biologically useful cross-sections for two photon photolysis. *Proc. Natl Acad. Sci. USA* **96,** 1193–1200 (1999).
14. Matsuzaki, M. *et al.* Dendritic spine geometry is critical for AMPA receptor expression in hippocampal CA1 pyramidal neurons. *Nature Neurosci.* **4,** 1086–1092 (2001).
15. Carter, A. G. & Sabatini, B. L. State-dependent calcium signaling in dendritic spines of striatal medium spiny neurons. *Neuron* **44,** 483–493 (2004).
16. Sobczyk, A., Scheuss, V. & Svoboda, K. NMDA receptor subunit-dependent [Ca^{2+}] signaling in individual hippocampal dendritic spines. *J. Neurosci.* **25,** 6037–6046 (2005).
17. Denk, W., Strickler, J. H. & Webb, W. W. Two-photon laser scanning microscopy. *Science* **248,** 73–76 (1990).
18. Svoboda, K. & Yasuda, R. Principles of two-photon excitation microscopy and its applications to neuroscience. *Neuron* **50,** 823–839 (2006).
19. Feng, G. *et al.* Imaging neuronal subsets in transgenic mice expressing multiple spectral variants of GFP. *Neuron* **28,** 41–51 (2000).
20. Sabatini, B. S., Oertner, T. G. & Svoboda, K. The life-cycle of Ca^{2+} ions in spines. *Neuron* **33,** 439–452 (2002).
21. Muller, W. & Connor, J. A. Dendritic spines as individual neuronal compartments for synaptic Ca^{2+} responses. *Nature* **354,** 73–76 (1991).
22. Kopec, C. D., Li, B., Wei, W., Boehm, J. & Malinow, R. Glutamate receptor exocytosis and spine enlargement during chemically induced long-term potentiation. *J. Neurosci.* **26,** 2000–2009 (2006).
23. Nusser, Z. *et al.* Cell type and pathway dependence of synaptic AMPA receptor number and variability in the hippocampus. *Neuron* **21,** 545–559 (1998).
24. Takumi, Y., Ramirez-Leon, V., Laake, P., Rinvik, E. & Ottersen, O. P. Different modes of expression of AMPA and NMDA receptors in hippocampal synapses. *Nature Neurosci.* **2,** 618–624 (1999).
25. Nimchinsky, E. A., Yasuda, R., Oertner, T. G. & Svoboda, K. The number of glutamate receptors opened by synaptic stimulation in single hippocampal spines. *J. Neurosci.* **24,** 2054–2064 (2004).
26. Lang, C. *et al.* Transient expansion of synaptically connected dendritic spines upon induction of hippocampal long-term potentiation. *Proc. Natl Acad. Sci. USA* **101,** 16665–16670 (2004).
27. Dan, Y. & Poo, M. M. Spike timing-dependent plasticity of neural circuits. *Neuron* **44,** 23–30 (2004).
28. Bi, G. Q. & Poo, M. M. Synaptic modifications in cultured hippocampal neurons: dependence on spike timing, synaptic strength, and postsynaptic cell type. *J. Neurosci.* **18,** 10464–10472 (1998).
29. Wittenberg, G. M. & Wang, S. S. Malleability of spike-timing-dependent plasticity at the CA3–CA1 synapse. *J. Neurosci.* **26,** 6610–6617 (2006).
30. Losonczy, A. & Magee, J. C. Integrative properties of radial oblique dendrites in hippocampal CA1 pyramidal neurons. *Neuron* **50,** 291–307 (2006).
31. Scanziani, M., Malenka, R. C. & Nicoll, R. A. Role of intercellular interactions in heterosynaptic long-term depression. *Nature* **380,** 446–450 (1996).
32. Schuman, E. M. & Madison, D. V. A requirement for the intercellular messenger nitric oxide in long-term potentiation. *Science* **254,** 1503–1506 (1991).
33. Gray, N. W., Weimer, R. M., Bureau, I. & Svoboda, K. Rapid Redistribution of synaptic PSD-95 in the neocortex *in vivo*. *PLoS Biol.* **4,** e370 (2006).
34. Tsuriel, S. *et al.* Local sharing as a predominant determinant of synaptic matrix molecular dynamics. *PLoS Biol.* **4,** e271 (2006).
35. Nishiyama, M., Hong, K., Mikoshiba, K., Poo, M. M. & Kato, K. Calcium stores regulate the polarity and input specificity of synaptic modification. *Nature* **408,** 584–588 (2000).
36. Royer, S. & Pare, D. Conservation of total synaptic weight through balanced synaptic depression and potentiation. *Nature* **422,** 518–522 (2003).
37. Frey, U. & Morris, R. G. Weak before strong: dissociating synaptic tagging and plasticity-factor accounts of late-LTP. *Neuropharmacology* **37,** 545–552 (1998).
38. Casadio, A. *et al.* A transient, neuron-wide form of CREB-mediated long-term facilitation can be stabilized at specific synapses by local protein synthesis. *Cell* **99,** 221–237 (1999).
39. Fonseca, R., Nagerl, U. V., Morris, R. G. & Bonhoeffer, T. Competing for memory: hippocampal LTP under regimes of reduced protein synthesis. *Neuron* **44,** 1011–1020 (2004).
40. Li, X. *et al.* Generation of destabilized green fluorescent protein as a transcription reporter. *J. Biol. Chem.* **273,** 34970–34975 (1998).
41. Abraham, W. C. & Bear, M. F. Metaplasticity: the plasticity of synaptic plasticity. *Trends Neurosci.* **19,** 126–130 (1996).
42. Turrigiano, G. G. & Nelson, S. B. Homeostatic plasticity in the developing nervous system. *Nature Rev. Neurosci.* **5,** 97–107 (2004).
43. Huang, Y. Y., Colino, A., Selig, D. K. & Malenka, R. C. The influence of prior synaptic activity on the induction of long-term potentiation. *Science* **255,** 730–733 (1992).
44. Golding, N. L., Staff, N. P. & Spruston, N. Dendritic spikes as a mechanism for cooperative long-term potentiation. *Nature* **418,** 326–331 (2002).
45. Holtmaat, A. J. *et al.* Transient and persistent dendritic spines in the neocortex *in vivo*. *Neuron* **45,** 279–291 (2005).

Supplementary Information is linked to the online version of the paper at www.nature.com/nature.

Acknowledgements We thank H. Zhong and R. Yasuda for discussions, T. O'Connor for programming assistance, K. H. Wang for *destabilized EGFP* DNA, and R. Malinow and J. Magee for comments on the manuscript. This work was supported by HHMI, by the NIH, and by a David and Fanny Luke Fellowship (C.D.H.).

Author Information Reprints and permissions information is available at www.nature.com/reprints. Correspondence and requests for materials should be addressed to K.S. (svobodak@janelia.hhmi.org).

METHODS

Preparation. Acute hippocampal brain slices (300 μm thick) from Thy1 GFP mice[19] (line M; postnatal day 14–18) were prepared in accordance with the animal care and use guidelines of Cold Spring Harbor Laboratory and Janelia Farm Research Campus. Slices were cut in gassed (95% O_2/5% CO_2), ice-cold cutting solution containing 110 mM choline chloride, 25 mM $NaHCO_3$, 25 mM D-glucose, 2.5 mM KCl, 7 mM $MgCl_2$, 0.5 mM $CaCl_2$, 1.25 mM NaH_2PO_4, 11.5 mM sodium ascorbate and 3 mM sodium pyruvate. Slices were then incubated in gassed artificial cerebral spinal fluid (ACSF) containing 127 mM NaCl, 25 mM $NaHCO_3$, 25 mM D-glucose, 2.5 mM KCl, 1 mM $MgCl_2$, 2 mM $CaCl_2$ and 1.25 mM NaH_2PO_4 at 35 °C for 30 min and then at room temperature (22–24 °C) until used.

Hippocampal slice cultures (Supplementary Figs 2 and 4) were prepared from postnatal day 6 or 7 rats[46], in accordance with institutional animal care and use guidelines. After 5–8 days in culture, cells were transfected by ballistic gene transfer using gold beads (~15 mg, 1.6 μm diameter) coated with 10 μg of plasmid DNA. Experiments were performed 2–3 days post-transfection.

Experiments were performed at room temperature except for those in Fig. 3 (33 °C). MNI-caged-L-glutamate, CPP, NBQX (2,3-dioxo-6-nitro-1,2,3,4-tetrahydrobenzo[f]quinoxaline-7-sulfonamide), thapsigargin and ryanodine were from Tocris; amphotericin B was from Sigma; and TTX (tetrodotoxin), anisomycin, emetine and cycloheximide were from Calbiochem.

Electrophysiology. Perforated patch-clamp recordings were used to prevent the washout of intracellular signalling molecules and LTP[28,47]. The internal solution contained 136.5 mM potassium gluconate, 17.5 mM KCl, 9 mM NaCl, 1 mM $MgCl_2$, 10 mM HEPES, 0.2 mM EGTA and 0.5 mg ml^{-1} amphotericin B. Pipettes were front-filled with a small volume of internal solution without amphotericin B. Perforations reached a stable series resistance (36 ± 8 MΩ, mean ± s.d.) within 30–45 min of seal formation. Series resistances were stable (±20%) throughout the experiment. uEPSCs were measured in response to test stimuli (0.1 Hz) at −70 mV. uEPSC amplitudes were measured as the difference between the mean current amplitude over a 5-ms window around the peak and the mean current amplitude over a 100-ms window before the uncaging stimulus. Each time point is the average of five trials (Fig. 1b, d, f and Fig. 4d–f). Spike-timing-dependent LTP (Fig. 4) was induced in current-clamp mode. Action potentials were triggered by brief current injections at the soma (2 ms, 1–3 nA). Voltage-clamp whole-cell recordings for [Ca^{2+}] imaging (Supplementary Fig. 1) were made using an internal solution containing 135 mM $CsMeSO_3$, 10 mM HEPES, 10 mM Na-phosphocreatine, 4 mM $MgCl_2$, 4 mM Na_2-ATP, 0.4 mM Na-GTP, 3 mM ascorbate, 0.03 mM Alexa 594 and 0.5 mM Fluo-4FF.

Synaptic stimulation (Fig. 3) was performed using short current pulses (0.1 ms, 30 μA) delivered with a glass pipette (~2–3 μm tip) filled with ACSF and 10 μM Alexa 594 to aid pipette placement. The pipette was positioned 10–20 μm from a GFP-labelled dendrite of interest. Each pulse produced an EPSP with amplitudes of 7.8 ± 2.7 mV ($n = 7$ stimulus positions from 3 cells, mean ± s.d., measured in parallel experiments), corresponding to the activation of ~30 synapses, a small subset of the synapses on typical CA1 pyramidal cells (total, ~10^4 synapses). The activated synapses are distributed throughout the dendritic tree, implying that multiple activated synapses are rarely found on a short stretch of dendrite[48,49]. We identified activated synapses that had undergone plasticity on the basis of spine enlargement. Image stacks containing a 30-μm-long stretch of dendrite were compared before and immediately after the synaptic LTP protocol (120 stimuli at 2 Hz, low extracellular Mg^{2+}). $\Delta F/F$ images (Fig. 3b) were generated after low-pass filtering and image alignment using cross-correlation analysis allowing for distortions. Spontaneous fluctuations in fluorescence intensity (that is, spine volume) in non-stimulated spines had a coefficient of variation of 0.21 ± 0.02. After the synaptic LTP protocol, spines that enlarged by more than three times the coefficient of variation of spontaneous fluctuations ($\Delta Vol > 60\%$) were scored as synaptic LTP spines. Structural plasticity after synaptic stimulation was sparse, consistent with the expected activation of a small subset of synapses. Of the 114 imaged dendrites, 16 contained at least one enlarged spine (range 1–2 spines). For 14 of these 16 dendrites, only a single spine in the field of view enlarged after synaptic stimulation. In the two cases where multiple spines enlarged, the spine receiving the subthreshold protocol was less than 12 μm from one, but not from the other, enlarged spine.

Imaging and glutamate uncaging. Two-photon imaging and glutamate uncaging were performed using a custom-built microscope with two Ti:sapphire lasers (910 nm for imaging GFP and 720 nm for uncaging; MaiTai, Spectra Physics) controlled by ScanImage[50], as described[51]. In brief, the intensity of each beam was controlled independently by electro-optical modulators (Pockels cells, Conoptics). The polarization angle was set using a half-wave plate. The beams were combined with a polarizing beam-splitting cube (CVI Laser Optics) and passed through the same set of scan mirrors and objective (×60, 0.9 NA; Olympus). To aid alignment, two steering mirrors were used for each beam. The upstream position-steering mirror adjusted the position of the beam at the back focal plane of the objective. The downstream angle-steering mirror (ASM) was placed in a conjugate plane to the scan mirrors and back focal plane of the objective using a Keplerian telescope consisting of two long focal-length plano-convex lenses. Adjustment of the ASM changed the angle, but not the position, of the beam at the back focal plane of the objective, thus moving the beam in the sample plane. Coarse alignment was first performed to center the beams at the back focal plane of the objective. For fine alignment at the sample plane, 0.1 μm fluorescent beads were imaged simultaneously with both beams. The ASMs were adjusted until the images overlapped. The *x*, *y* and *z* resolutions (full-width at half-maximum) for the imaging beam (910 nm) were 0.53 μm, 0.59 μm and 1.89 μm, respectively. For the uncaging beam (720 nm), the *x*, *y* and *z* resolutions (full-width at half-maximum) were 0.50 μm, 0.56 μm and 1.66 μm, respectively.

Green and red fluorescence photons were separated using a dichroic mirror (565 nm) and bandpass filters (510/70, 635/90; Chroma). Photons were collected using photomultiplier tubes (Hamamatsu R3896 except for the epifluorescence green signal, which was collected using Hamamatsu H7422-40). Epi- and trans-fluorescence signals were collected and summed[52].

For glutamate uncaging, 2.5 mM MNI-caged-L-glutamate was added to the ACSF. Only spines well separated from both the dendrite and neighbouring spines were selected for experiments. The laser beam was parked at a manually determined uncaging location approximately 0.5 μm from the tip of the spine head in the direction away from the parent dendrite. The uncaging location was readjusted between uEPSC amplitude time points (5 test pulses per time point, 0.1 Hz; 5 min between time points), but not between test pulses (Figs 1b, d, f and 4d–f). The uncaging location was also repositioned after spine enlargement. To assess the accuracy of manual positioning, we compared uEPSC amplitudes across baseline time points for all spines (LTP, sub and nearby spines). uEPSC amplitudes were not significantly different between time points (repeated measures ANOVA, $P = 0.25$); similarly, trial-to-trial fluctuations were not different for test pulses within a time point and between time points (*t*-test, $P = 0.5$). Manual repositioning therefore did not affect the measurement of uEPSC amplitude nor did it contribute significantly to uEPSC amplitude fluctuations.

For test pulses, 45 mW laser power was delivered to the back focal aperture of the objective for 1 ms. During stimulus trains, we used 20-mW pulses lasting 4 ms for the LTP protocol and lasting 1 ms for the subthreshold protocol. For spike-timing-dependent LTP, all uncaging pulses were 1 ms in duration with 45 mW laser power at the back focal aperture of the objective. Approximately 20% of this laser power was transmitted through the objective. Initial spine volumes were indistinguishable across conditions (data not shown). The distances between spines tested for uEPSC changes were similar on average (Fig. 1: LTP protocol only, 3.1 ± 0.4 μm; subthreshold protocol only, 2.6 ± 0.6 μm; crosstalk, 3.5 ± 0.2 μm; ANOVA, $P > 0.7$. Figure 4: $\Delta t = 5$ ms, 2.2 ± 0.3 μm; $\Delta t = 35$ ms, 2.3 ± 0.4 μm; crosstalk, 2.3 ± 0.2 μm; ANOVA, $P > 0.95$). The depth in the slice was restricted to 25–50 μm.

Plasticity was induced using four protocols: depolarization to ~0 mV in perforated patch-clamp mode paired with 30 uncaging pulses at 0.5 Hz in 2 mM Ca^{2+}, 1 mM Mg^{2+} and 1 μM TTX (Fig. 1); 30 uncaging pulses at 0.5 Hz in 4 mM Ca^{2+}, 0 mM Mg^{2+} and 1 μM TTX (Fig. 2); 120 synaptic stimuli at 2 Hz in 4 mM Ca^{2+} and 0 mM Mg^{2+} at 33 °C (Fig. 3); and an uncaging pulse followed by 3 action potentials at 50 Hz, repeated 60 times at 2 Hz in 2 mM Ca^{2+} and 1 mM Mg^{2+} in perforated patch-clamp mode (Fig. 4). The time window (Δt) for spike-timing-dependent LTP was defined as the time between the uncaging pulse and the first action potential.

[Ca^{2+}] imaging was performed as described[49]. Images were acquired every 64 ms in frame-scan mode. [Ca^{2+}] transients were measured as the change in Ca^{2+}-sensitive green fluorescence (500 μM Fluo-4FF; ΔG) divided by the Ca^{2+}-insensitive red fluorescence (30 μM Alexa 594; *R*), normalized to $(G/R)_{max}$ measured in 10 mM Ca^{2+}.

Controls for inhibitor function. To test the efficacy of thapsigargin and ryanodine (Supplementary Fig 3), a CA1 cell in an acute hippocampal slice was filled with 500 μM Fluo 4FF and 30 μM Alexa 594. Caffeine (40 mM in ACSF) was pressure-applied for 2 sec from a pipette located ~20 μm from the soma of the filled cell[53]. Caffeine-induced [Ca^{2+}] transients in the soma were measured before and 5 min after the application of 1 μM thapsigargin and 20 μM ryanodine.

To test protein synthesis inhibitor function (Supplementary Fig 4), cells in cultured rat hippocampal slices were transfected with destabilized EGFP[40]. Slices were incubated in ACSF at room temperature. Changes in green fluorescence intensity in the thick apical dendrite were monitored following application of DMSO (0.1 %), 25 μM anisomycin, 60 μM cycloheximide or 50 μM emetine.

Data analysis. Spine volumes were measured as the integrated green fluorescence after background subtraction, which is proportional to spine volume[45], normalized to the fluorescence intensity of the thick apical dendrite[25]. The origin of all time axes corresponds to the start of the uncaging protocols. Volume changes at nearby spines (Figs 1–4) were averaged across all neighbouring spines less than 4 μm from the LTP or sub spines. uEPSC changes at nearby spines (Figs 1 and 4) were from an individual neighbouring spine for each experiment. In the bar graphs, ΔVol and ΔuEPSC were normalized to the baseline and measured starting 15 min post stimulus until the end of the time course.

All data are presented as mean ± s.e.m. unless noted otherwise. *n* indicates the number of spines analysed. One experiment was performed per cell, except to map the spike-timing-dependent LTP time window for which up to three experiments per cell were performed sequentially. Each figure summarizes all experiments, except for Fig. 3 in which only experiments with a scored synaptic LTP spine in the field-of-view were analysed.

P values are from two-tailed *t*-tests unless noted otherwise. For all *t*-tests the null hypothesis stated that the mean was equal to zero, except for pharmacology experiments in which the null hypothesis stated that the means of control and drug conditions were the same.

46. Stoppini, L., Buchs, P. A. & Muller, D. A. A simple method for organotypic cultures of nervous tissue. *J. Neurosci. Methods* **37,** 173–182 (1991).
47. Yasuda, R. *et al.* Supersensitive Ras activation in dendrites and spines revealed by two-photon fluorescence lifetime imaging. *Nature Neurosci.* **9,** 283–291 (2006).
48. Oertner, T. G., Sabatini, B. S., Nimchinsky, E. A. & Svoboda, K. Facilitation at single synapses probed with optical quantal analysis. *Nature Neurosci.* **5,** 657–664 (2002).
49. Yasuda, R. *et al.* Imaging calcium concentration dynamics in small neuronal compartments. *Sci. STKE* **2004,** pl5 (2004).
50. Pologruto, T. A., Sabatini, B. L. & Svoboda, K. ScanImage: flexible software for operating laser-scanning microscopes. *Biomed. Eng. Online* **2,** 13 (2003).
51. Pologruto, T. A. *Imaging neural activity and [Ca^{2+}] with genetically encoded calcium indicators and two-photon excitation laser scanning microscopy.* PhD thesis, Harvard Univ. (2004).
52. Mainen, Z. F. *et al.* Two-photon imaging in living brain slices. *Methods* **18,** 231–239 (1999).
53. Garaschuk, O., Yaari, Y. & Konnerth, A. Release and sequestration of calcium by ryanodine-sensitive stores in rat hippocampal neurones. *J. Physiol.* **502,** 13–30 (1997).

Supplementary Notes

Spine Ca^{2+} signals produced by glutamate uncaging

We imaged uncaging-evoked [Ca^{2+}] transients in neurons loaded with a green Ca^{2+}-sensitive indicator (G; 500 μM Fluo 4FF) and a red Ca^{2+}-insensitive dye (R; 30 μM Alexa 594) (Supplementary Fig 1a). To calculate [Ca^{2+}] from fluorescence measurements, we used the relationship:

$$\frac{G/R}{(G/R)_{\max}} = \frac{[Ca^{2+}]}{K_D + [Ca^{2+}]} \quad \text{(ref. 1)}$$

where $(G/R)_{max}$ is the green-to-red fluorescence ratio at saturating [Ca^{2+}] and the dissociation constant, K_D, of Fluo 4FF is 10.4 μM (ref. 1).

The presence of Ca^{2+}-sensitive indicators increases the cytoplasmic buffer capacity (κ) and decreases the amplitudes of [Ca^{2+}] transients (Δ[Ca^{2+}]) (ref. 1). The endogenous buffer capacity (κ_E) for hippocampal spines is ~ 20 (ref. 2). The added buffer capacity due to the presence of [Ca^{2+}] indicator (κ_{dye}) can be calculated as:

$$\kappa_{dye} = \frac{K_D[B]_{total}}{(K_D + [Ca^{2+}])^2} \quad \text{(ref. 1)}$$

where $[B]_{total}$ is the total buffer concentration. Therefore 500 μM Fluo 4FF adds a buffer capacity of $\kappa_{dye} \sim 50$.

NMDA receptor-mediated [Ca^{2+}] accumulations can be described as:

$$\Delta[Ca^{2+}] = \frac{Q\beta^{-1}}{V_{sp}(1-\Gamma\beta^{-1}\tau_{NMDA})}\left[\exp\left(-\frac{\Gamma t}{\beta}\right) - \exp\left(-\frac{t}{\tau_{NMDA}}\right)\right] \quad \text{(ref. 1)}$$

where Q is the total amount (moles) of Ca^{2+} influx, V_{sp} is the volume of the spine, Γ is the extrusion rate constant (1600 s^{-1}) (ref. 2), τ_{NMDA} is the decay time constant of the NMDA receptor-mediated current (~ 100 ms; Supplementary Fig. 1a), and $\beta = (1 + \kappa_E + \kappa_{dye})$. The time of peak [$Ca^{2+}$] accumulation, t_{peak}, can be calculated as:

$$t_{peak} = \frac{\ln\left(\frac{\beta}{\Gamma\tau_{NMDA}}\right)}{-\frac{\Gamma}{\beta} + \frac{1}{\tau_{NMDA}}}$$

Therefore, peak [Ca^{2+}] accumulations are expected to be reduced by a factor of ~ 1.4 due to the presence of the Ca^{2+} indicator.

Peak uncaging-evoked [Ca^{2+}] accumulations during the LTP protocol in low extracellular Mg^{2+} and 4 mM extracellular Ca^{2+} were ~ 3.3 μM (Supplementary Fig 1c), corresponding to ~ 4.6 μM in the absence of indicator. This value is smaller than the Ca^{2+} concentrations measured during low-frequency synaptic stimulation at 0 mV (ref. 2) and is therefore in a physiological range. During the subthreshold protocol, peak [Ca^{2+}] accumulations were ~ 0.7 μM (Supplementary Fig 1c), corresponding to ~ 1.0 μM in the absence of indicator.

At a postsynaptic potential of ~ 0 mV in 2 mM extracellular Ca^{2+} and 1 mM extracellular Mg^{2+}, peak [Ca^{2+}] accumulations during the LTP protocol were ~ 1.8 μM (Supplementary Fig 1c), or ~ 2.5 μM without exogenous buffer. During the subthreshold protocol, peak [Ca^{2+}] accumulations were ~ 0.3 μM (Supplementary Fig 1c), corresponding to ~ 0.4 μM in the absence of indicator.

Uncaging pulses did not produce detectable [Ca^{2+}] accumulations in nearby spines (< 3 μm from the stimulated spine, mean distance = 1.7 ± 0.4 μm), either in low extracellular Mg^{2+} ($\Delta[Ca^{2+}]_{\text{nearby spine, LTP pulse}}$ = 0.03 ± 0.04 μM, $P > 0.6$; $\Delta[Ca^{2+}]_{\text{nearby spine, sub pulse}}$ = 0.02 ± 0.04 μM, $P > 0.7$) or at a postsynaptic potential of ~ 0 mV ($\Delta[Ca^{2+}]_{\text{nearby spine, LTP pulse}}$ = 0.02 ± 0.03 μM, $P > 0.6$; $\Delta[Ca^{2+}]_{\text{nearby spine, sub pulse}}$ = 0.01 ± 0.04 μM, $P > 0.9$) (Supplementary Fig 1c). These data show that uncaging-evoked [Ca^{2+}] accumulations were restricted to the stimulated spine. Because [Ca^{2+}] imaging can detect the activation of individual NMDA-Rs[3], these data further indicate that glutamate did not diffuse over intersynaptic distances to stimulate nearby spines. Finally, our [Ca^{2+}] measurements were performed with high concentrations of exogenous buffer, which prolongs the time course and thus promotes the spatial spread of the [Ca^{2+}] signal[2]. All plasticity experiments (Figs 1-6, Supplementary Fig 2) were performed without exogenous Ca^{2+} buffer and therefore will show even greater compartmentalization of Ca^{2+}.

Glutamate-independent effects of uncaging

Uncaging generates diffusible photoproducts in addition to glutamate, including protons that locally decrease the extracellular pH[4]. We tested if the uncaging process and its non-glutamate photoproducts contribute to crosstalk. We applied the LTP protocol (30 pulses at 0.5 Hz, 4 ms pulse duration; see Fig 1) at a single spine (LTP spine) at a postsynaptic potential of ~ -70 mV, preventing the induction of LTP. Ninety seconds later we applied the subthreshold protocol (30 pulses at 0.5 Hz, 1 ms pulse duration; see Fig1) at a nearby spine (sub spine), at ~ 0 mV. Under these conditions uEPSC amplitudes and spine volumes did not change at either spine ($\Delta uEPSC_{LTP\ spine}$ = -8 ± 6 %, $P > 0.3$; $\Delta uEPSC_{sub\ spine}$ = -6 ± 8 %, $P > 0.6$; $\Delta vol_{LTP\ spine}$ = -4 ± 5 %, $P > 0.5$; $\Delta vol_{sub\ spine}$ = 3 ± 7 %, $P > 0.7$). Non-glutamate photoproducts generated by uncaging therefore did not induce LTP, spine enlargement, or crosstalk. Also, LTP induction and spine enlargement required the pairing of uncaging and postsynaptic depolarization, supporting the involvement of NMDA-Rs (Fig 6b). Finally, these results argue that crosstalk is triggered by LTP induction.

References

1. Yasuda, R. et al. Imaging calcium concentration dynamics in small neuronal compartments. *Sci STKE* **2004**, pl5 (2004).
2. Sabatini, B.S., Oertner, T.G. & Svoboda, K. The life-cycle of Ca^{2+} ions in spines. *Neuron* **33**, 439-452 (2002).
3. Nimchinsky, E.A., Yasuda, R., Oertner, T.G. & Svoboda, K. The number of glutamate receptors opened by synaptic stimulation in single hippocampal spines. *J Neurosci* **24**, 2054-2064 (2004).
4. Canepari, M., Nelson, L., Papageorgiou, G., Corrie, J.E. & Ogden, D. Photochemical and pharmacological evaluation of 7-nitroindolinyl-and 4-methoxy-7-nitroindolinyl-amino acids as novel, fast caged neurotransmitters. *J Neurosci Methods* **112**, 29-42. (2001).

Supplementary Figure 1

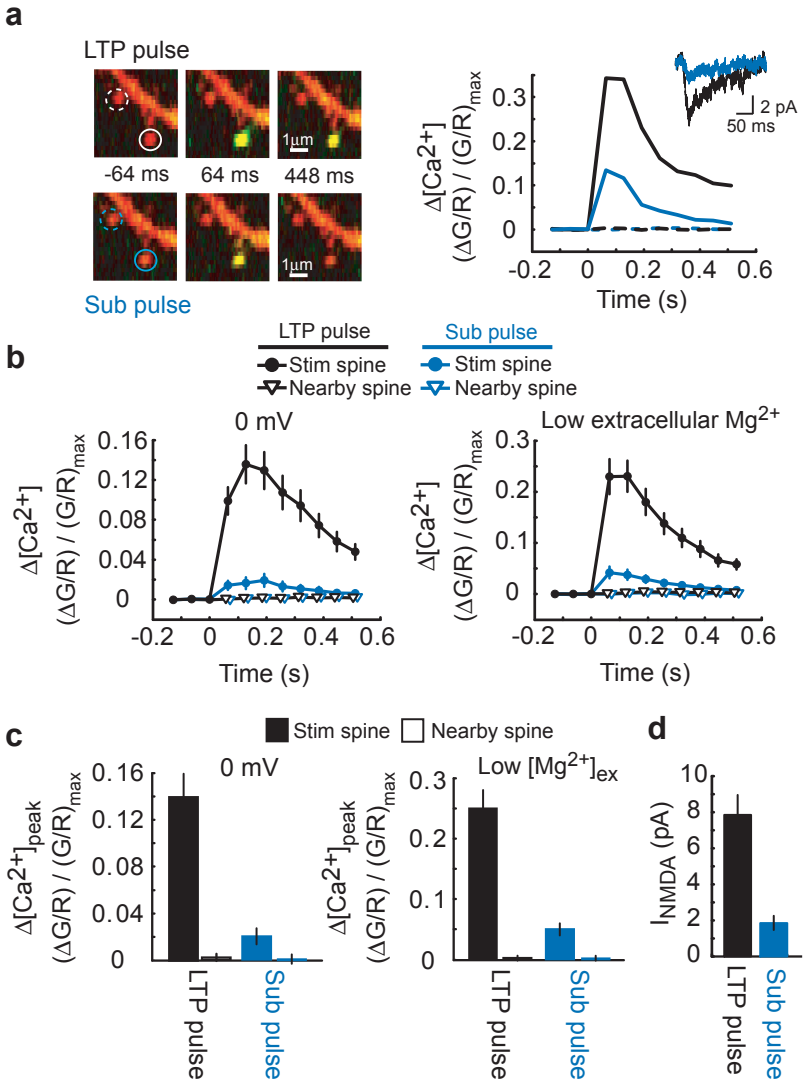

Supplementary Figure 1 | Characterization of glutamate uncaging pulses. a, Left panels, example [Ca^{2+}] images for individual pulses from the LTP (4 ms pulse duration) and subthreshold (1 ms pulse duration) protocols in low extracellular Mg^{2+}. The cell was filled with a red Ca^{2+}-insensitive dye (R; 30 μM Alexa 594) and a green Ca^{2+}-sensitive dye (G; 500 μM Fluo 4FF). At time = 0, a single uncaging pulse was given at the spine marked by the solid circle. Right panels, time-course of uncaging-evoked [Ca^{2+}] transients triggered by LTP pulses (black) and subthreshold pulses (blue) in the stimulated (solid line) and nearby spines (dashed line). Example NMDA-R currents (averaged over 5 trials) are shown. **b,** [Ca^{2+}] transients in stimulated and nearby spines for LTP or subthreshold pulses at 0 mV (left; in 2 mM extracellular Ca^{2+} and 1 mM extracellular Mg^{2+}; n = 14 spines from 3 cells) and in low extracellular Mg^{2+} (right; at -70 mV in 4 mM extracellular Ca^{2+} and nominally 0 mM extracellular Mg^{2+}; n = 18 spines from 3 cells, mean ± sem). **c,** Peak [Ca^{2+}] accumulations in stimulated and nearby spines for LTP and subthreshold pulses at 0 mV or in low extracellular Mg^{2+}. Data are from (b). **d,** NMDA-R currents for the LTP and subthreshold pulses in low extracellular Mg^{2+}. NBQX (10 μM) was added to isolated NMDA-R currents. n = 18 spines from 3 cells, mean ± sem.

Supplementary Figure 2

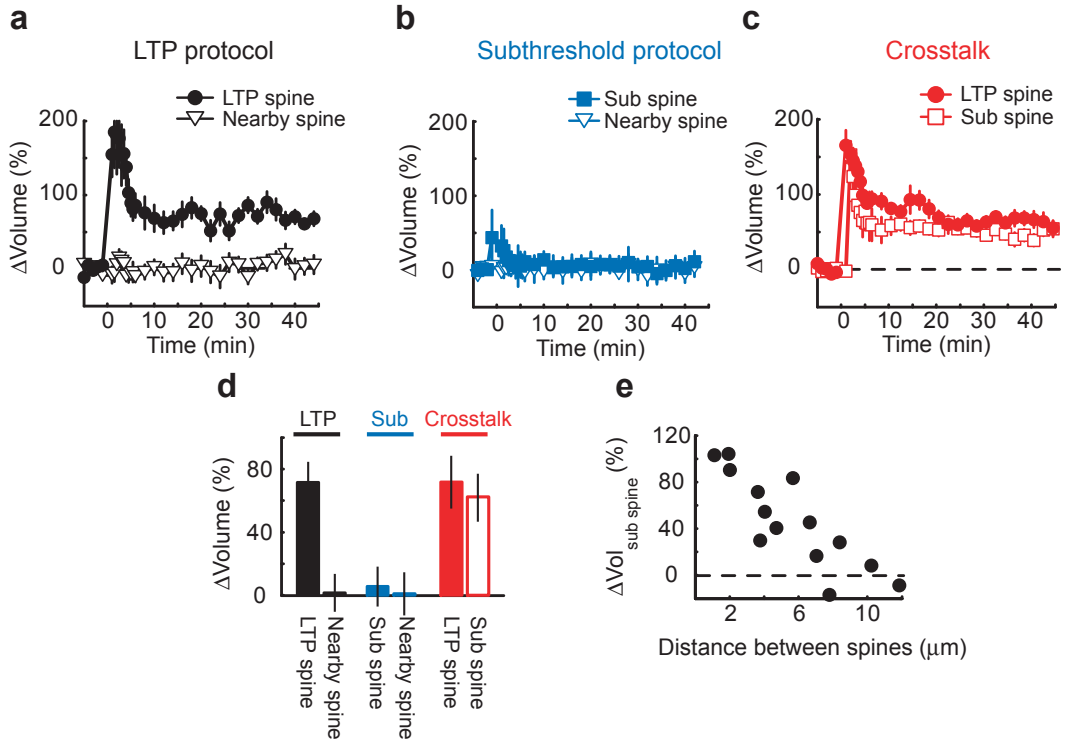

Supplementary Figure 2 | Crosstalk in cultured rat hippocampal slices. a, Time-course of the spine volume changes induced by the LTP protocol in GFP-expressing CA1 cells. At time = 0 the LTP protocol was applied to the LTP spine (in low extracellular Mg^{2+}). n = 6, mean ± sem. **b,** Time-course of the spine volume changes induced by the subthreshold protocol. At time = 0 the subthreshold protocol was applied to the sub spine (in low extracellular Mg^{2+}). n = 5, mean ± sem. **c,** Time-course of the spine volume changes for the crosstalk case. At time = 0 the LTP protocol was applied to the LTP spine and, 90 seconds later, the subthreshold protocol was given at a nearby spine (sub spine). n = 6, mean ± sem. **d,** Spine volume changes for the LTP protocol only, the subthreshold protocol only, and the crosstalk cases. Error bars indicate mean ± sem. **e,** Length scale of crosstalk. The LTP protocol was applied to the LTP spine and, 90 seconds later, the subthreshold protocol was applied to a neighboring spine (sub spine).

Supplementary Figure 3

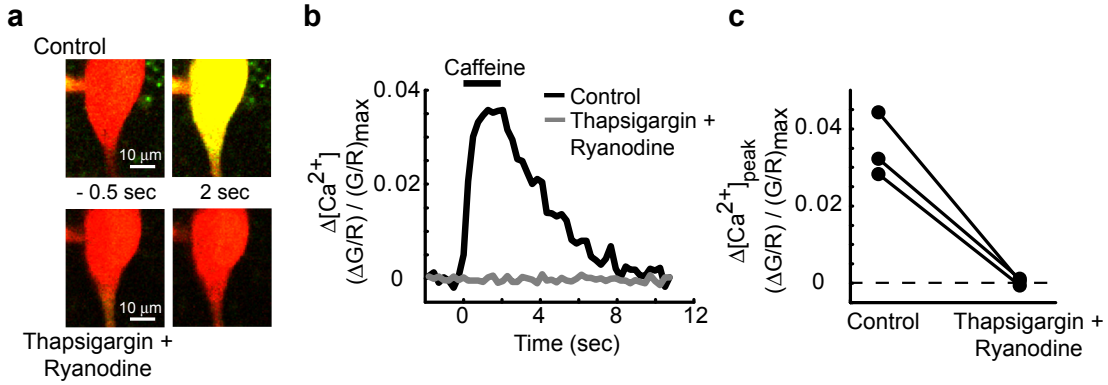

Supplementary Figure 3 | Control for thapsigargin and ryanodine function. a, Example [Ca^{2+}] images before and after caffeine application in the presence or absence of 1 µM thapsigargin and 20 µM ryanodine. The cell was filled with a red (R) Ca^{2+}-insensitive dye (30 µM Alexa 594) and a green (G) Ca^{2+}-sensitive indicator (500 µM Fluo 4FF). At time = 0, caffeine (40 mM) was pressure applied onto the soma for 2 seconds. **b,** Caffeine-induced [Ca^{2+}] transients for the example shown in (a). **c,** Peak caffeine-induced [Ca^{2+}] accumulations before and after application of thapsigargin and ryanodine. n = 3, $p < 0.01$.

Supplementary Figure 4

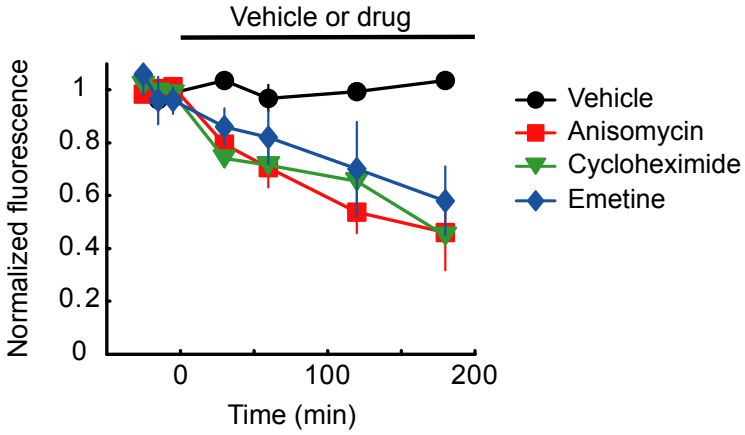

Supplementary Figure 4 | Control for protein synthesis inhibitor function. Time-course of the normalized fluorescence intensity of destabilized EGFP in the thick apical dendrite in the presence of vehicle (0.1% DMSO), 25 µM anisomycin, 60 µM cycloheximide, and 50 µM emetine. For each condition, n = 2, mean ± sem